A COMPARATIVE STUDY ON CONVERSION OF INDUSTRIAL COAL BY-PRODUCTS IN LOW SiO_2 ZEOLITE OF FAUJASITE TYPE

ESTUDIO COMPARATIVO SOBRE LA CONVERSIÓN DE SUBPRODUCTOS DE LA INDUSTRIA DEL CARBÓN EN ZEOLITA BAJA EN SiO_2 DE TIPO FAUJASITA

JENNY ANDREA OVIEDO VILLAMIZAR

Química MSc, Escuela de Química, Universidad Industrial de Santander, Bucaramanga, Colombia,, jaoviedo86@hotmail.com

JOSE ANTONIO HENAO MARTINEZ

Químico PhD, Profesor Titular, Escuela de Química, Universidad Industrial de Santander, Bucaramanga, Colombia, jahenao@uis.edu.co

CARLOS ALBERTO RIOS REYES

Geólogo PhD, Profesor Titular, Escuela de Geología, Universidad Industrial de Santander, Bucaramanga, Colombia, carios@uis.edu.co

Received for review December 6 th, 2011, accepted July 23th, 2012, final version August, 21 th, 2012

ABSTRACT: Colombian industrial coal by-products were evaluated as raw materials in laboratory-scale synthesis of faujasite-type low-SiO_2 zeolite of using an alkaline fusion step followed by hydrothermal treatment under various experimental conditions. By fusion with NaOH followed by hydrothermal reaction, coal by-products were converted into faujasite-type zeolite. The process of faujasite formation is discussed.

KEYWORDS: coal by-products, synthesis, zeolitic materials, hydrothermal, fusion

RESUMEN: Subproductos de carbón industrial colombiano fueron evaluados como materias primas para la síntesis a escala de laboratorio de zeolita baja en SiO_2 de tipo faujasita usando una etapa de fusión alcalina seguida por el tratamiento hidrotérmico en diferentes condiciones experimentales. La fusión con NaOH seguida de la reacción hidrotérmica promovió la conversión de los sub-productos de carbón en zeolita de tipo faujasita. El proceso de formación de faujasita se discute.

PALABRAS CLAVE: sub-productos de carbón, síntesis, materiales zeolíticos, hidrotermal, fusión

1. INTRODUCTION

Annually, coal industry worldwide produces millions of metric tons of by-products. However, only small portions of these materials are used beneficially, being landfilled as solid wastes. Furthermore, the amount of discharged material is expected to increase dramatically in the future. Due to increasing landfill costs, stricter environmental regulations, and the current interest in sustainable development, the effective recycling of industrial wastes for the production of products of greater value to mitigate the depletion of resources and environmental impact has become an increasing concern. The major application of solid wastes is for manufacturing of construction materials, where it can provide both technological and economic benefits. Therefore, zeolite synthesis from coal by-products like natural clinker (NC) and fly ash (FA) by several methods has been receiving a lot of attention. Since the pioneering works of Höller and Barth-Wirsching [1] and Ríos et al. [2] who were the first researchers that synthesized zeolites from FA and NC, respectively, much investigation has been conducted to convert these coal by-products to zeolites. The conversion of coal by-products into zeolites can be conventionally developed by hydrothermal crystallization under alkaline conditions, which has been reported by different authors [1–16]. Recently, the conventional alkaline conversion of these materials has been improved by using more sophisticated treatments [17–23]. The synthesis of zeolites from coal by-products in forms suitable for industrial applications is of great importance, mainly as ion exchangers, molecular

sieves, adsorbents, and catalysts. The resultant zeolitic materials have great potential to be developed as high-efficiency low-cost adsorbents with applications in environmental problems [24–27]. Zeolitic materials are highly selective scavengers of a variety of heavy metals that can be removed from liquid effluents through the process of ion exchange. In this paper, we investigate the synthesis of zeolites from coal by-products on a laboratory scale via the dissolution of alkali-fused aluminosilicate salts in water followed by hydrothermal treatment. Several parameters were selected: the alkaline activator/coal by-product ratio for a fusion of 1.2, fusion temperature and time 600 ºC and 1 h, respectively, the H_2O/alkali fused coal by-product ratio = 5 mL/g. The variables were: reaction time (6, 12, 24, 48, 72, and 96 h), and temperature (65, 80, and 95 °C).

2. EXPERIMENTAL PROCEDURE

2.1. Materials

The starting materials used for the synthesis of faujasite-type low-SiO_2 zeolite was supplied as follows: FA by the Termozipa Power Station, Cundinamarca (Colombia) and NC associated with the spontaneous combustion of coal seams from the late Paleocene Cerrejón Formation, which was collected from an open pit of the Cerrejón coal mining site, situated in La Guajira State (Colombia). They were prepared prior to synthesis, using the following steps: rough crushing with a Retsch Jaw Crusher BB 200 to ~ 2mm, milling with a Retsch RM100 mortar grinder mill to clay particle size and sieving with a 200 mesh Ro-Tap sieve shaker; 63 μm particles were selected for zeolite synthesis. The reagents used to activate these coal by-products were sodium hydroxide, NaOH, as pellets (99%, from Aldrich Chemical Company, Inc.), and distilled water using standard purification methods.

2.2. Zeolite synthesis

The synthesis of faujasite-type zeolite was investigated by using an alkaline fusion step prior to hydrothermal treatment. Optimal conditions for the synthesis of zeolites from coal by-products with a maximum value of cation exchange capacity are a coal by-product/alkaline activator ratio of 1:1.2 [17–18]. Therefore, alkali hydroxide powder was dry mixed with the coal by-product with this ratio for 30 min and the resultant mixture was calcined at 600 °C for 1 h [18]. The alkaline reagent added to the starting material acts as an activator agent during fusion. The alkali-fused products were then dissolved in water (H_2O/alkali fused starting material ratio = 5 mL/g), generally under stirring conditions until the reaction gels were homogenized aged for 24 h under static conditions. The mixtures were transferred into polytetrafluoroethylene (PTFE) bottles of 65 ml and then crystallized under static conditions at 65, 80, and 95 °C for 6, 12, 24, 48, 72, and 96 h.

2.3. Characterization

The mineral phases in the raw materials and as-synthesized products were studied by X-ray diffraction using a RIGAKU D/MAX IIIB diffractometer operating in Bragg-Brentano geometry with Cu-α1 radiation (λ = 1.5406 Å) at 40 kV and 20 mA and graphite monochromation. The scan parameters were step size 0.02°, dwell time 12 sec, and 2θ range 2–70°. Phase identification was performed by the Hanawalt method using the crystallographic database Powder Diffraction File (PDF-2) from the International Centre for Diffraction Data (ICDD). Full-pattern Rietveld refinement using the RIQAS 3.1 program (MDI Inc.) was performed to quantify the amounts of phases in NC and as-synthesized products. The chemical composition of the raw materials was investigated by X-ray fluorescence in a Shimazu EDX 800 HS XRF spectrometer. The quantification of the elements was carried out using the method of fundamental parameters (FP) with the software DXP-700E Version 1.00 Rel. 014. The morphology of the raw materials and as-synthesized zeolites was examined by environmental scanning electron microscopy (FEI Quanta 200), under the following analytical conditions: magnification = 100–6000x, WD = 7.0 mm, HV = 8.4 kV, spot = 3.0, signal = SE, detector = LFD.

3. RESULTS AND DISCUSSION

3.1. Chemical and mineralogical analyses of raw materials

Chemical composition has an important influence both on the potential application of raw materials and on the environmental impact of its subsequent use. Industrial coal by-products do not exhibit hazardous

characteristics, although specially-designed landfills are required to prevent the possible leaching of trace elements which affect water sources from them. The chemical composition of raw materials used in this study is presented in Table 1.

Table 1. Chemical composition of the raw materials

	Oxide weight (%)									
	SiO_2	Al_2O_3	Fe_2O_3	MgO	K_2O	CaO	TiO_2	Na_2O	P_2O_5	SO_3
NC	68,151	19,441	5,935	2,328	1,548	1,073	0,955	0,216	0,163	0,043
FA	60,115	26,409	5,719	0,434	1,815	0,567	1,302	0,000	0,459	2,965

The SiO_2/Al_2O_3 ratio is an important parameter for zeolite synthesis. Both NC and FA present appropriate SiO_2/Al_2O_3 ratios to be used as starting materials for the synthesis of low-Si zeolitic materials with a high cation exchange capacity. SiO_2/Al_2O_3 ratios are important for predicting the success in the process of zeolite synthesis, although it is also important to consider the occurrence of impurities in the starting material [28].

According to Ríos and co-workers [2,27–29], the chemical composition of the raw NC displays variations of up to 15 wt% among its major oxides (SiO_2, Al_2O_3, K_2O, and CaO), which probably reflects local heterogeneity related to small changes in the original sedimentary rock. NC has very high contents of SiO_2 (68.15%) and Al_2O_3 (19.44%) with a SiO_2/Al_2O_3 ratio = 3.5. NC shows very low contents of Ca and S, and a high content of Fe associated with the presence of hematite, which is very important taking into account that Fe-bearing minerals, mainly magnetite, can show an inert behaviour and Ca-bearing phases can act as a zeolite synthesis inhibitor through the formation of calcium silicate hydrate phases [9]. Raw FA has $\geq$70% of SiO_2+Al_2O_3+Fe_2O_3, with a SiO_2/Al_2O_3 ratio = 2.3, and very low contents of major impurities, such as Fe, Ca, and S. Therefore, it can be classified as a low-calcium Class F FA. According to Vassilev and Vassileva [30], it is commonly produced from the burning of higher-rank bituminous coals and anthracites and, therefore, this type of FA is pozzolanic in nature (hardening when reacted with $Ca(OH)_2$ and water). It can be also classified as a Sialic FA type [30]. The properties and chemical composition of FA vary according to coal source and power plant operation, which makes FAZs even more versatile.

A quantitative analysis was useful to accurately determine the proportion of each phase and to simultaneously express the particular characteristics of each phase, such as the crystalline system, space group, and cell constants [31].

Table 2 summarizes the best structural models used for refinement the X-ray diffraction (XRD) profiles of the raw materials. Models were selected in the qualitative analysis by using the PDF-2 of the International Centre for Diffraction Data (ICDD), as well as crystalline system, space group, atomic positions, and cell constants.

Table 3 shows the crystallographic data and the quantitative analysis of the phases obtained according to the models used in the refinement of the raw materials.

Table 2. Crystallographic data of the models used in the refinement of the raw materials

	ICSD	Crystalline system	Space group	a (Å)	b (Å)	c (Å)	α (°)	β (°)	γ (°)	V (Å3)	ρ (g/cm3)	Z
Qtz	200721	Trigonal	P3121	4.9148 (5)	4.9148 (5)	5.4062 (9)	90	90	120	113.09	2.65	3
Qtz	174	Trigonal	P3221	49.134	49.134	54.052	90	90	120	113.01	2.65	3
Mc	38135	Triclinic	C-1	85.784	12.96	72.112	89.7	115.967	90.875	720.69	2.56	4
Mul	43298	Ortorrombic	Pbam	7.584 (3)	7.693 (3)	2.890 (1)	90	90	90	168.61	3.1	2
Mag	84611	Cubic	Fd-3mz	8.375 (2)	8.375 (2)	8.375 (2)	90	90	90	587.43	5.23	8
Hem	64599	Trigonal	R-3cH	5.0285 (7)	5.0285 (7)	13.736 (2)	90	90	120	300.79	5.29	6
Hem	22505	Trigonal	R-3cH	5.0342 (3)	5.0342 (3)	13.7483 (4)	90	90	120	301.75	5.27	6
Mnt	(VIANI, 2002)	Triclinic	C2/m	5.18	8.98	15.00	90	90	90			

Table 3. Refinement data of the raw materials

			NC				FA			
			Low Qtz	Mc (int)	Ca-Mnt	Hem	Mul	Qtz	Mag	Hem
ICSD			200721	38135	----	64599	43298	174	84611	22505
Variables refinadas			52				41			
a (Å)			4.91556 (8)	8.536 (2)	5.16 (1)	5.0320 (1)	7.5674 (9)	4.9183 (3)	8.3613 (5)	4.832 (5)
b (Å)			4.91556 (8)	12.939 (2)	8.936 (5)	5.0320 (1)	7.694 (1)	4.9183 (3)	8.3613 (5)	4.832 (5)
c (Å)			5.4060 (2)	7.223 (1)	15.59 (1)	13.7358 (9)	2.8861 (2)	5.4077 (8)	8.3613 (5)	14.72 (4)
α (°)			90	89.16 (2)	90	90	90	90	90	90
β (°)			90	116.17 (1)	90	90	90	90	90	90
γ (°)			120	91.94 (2)	90	120	90	120	90	120
V ($Å^3$)			113.125 (5)	715.7 (2)	719 (2)	301.21 (2)	168.05 (3)	113.28 (2)	584.55 (6)	297.8 (9)
ρ (g/cm^3)			2.646	2.583	1.839	5.282	3.109 (1)	2.642 (1)	5.262 (1)	5.34 (2)
FWHM	Low angle	U	0.11 (1)	0.000000	0.000000	0.18 (1)	0.275032	0.993169	0.000000	0.000000
		V	-0.08 (1)	0.036612	0.000000	-0.135 (5)	-0.186870	-0.15 (1)	0.000000	0.000000
		W	0.040 (2)	0.095048	1.82 (4)	0.035225	0.069 (2)	0.048217	0.158921	0.653510
	High angle	U	0.04 (1)				0.225802	0.45 (2)		
		V	-0.006 (8)				-0.187340	-0.229 (7)		
		W	0.006 (1)				0.059 (1)	0.048217		
RB (%)			3.36	11.67	5.90	7.63	8.31	5.50	8.31	5.50
RP (%)			7.47				10.76			
RWP (%)			18.66				16.11			
Ajuste de bondad (GOF)			2.00				1.39			
% DRX (Cuantitativo)*			25.4	14.2	11.1	3.3	15.8	11.6	0.9	0.6
*Amorfo			46				71			

Figure 1 illustrates the refinement for the starting materials. In black, the experimental XRD pattern; in red, the calculated XRD pattern; in green, the amorphous phase.

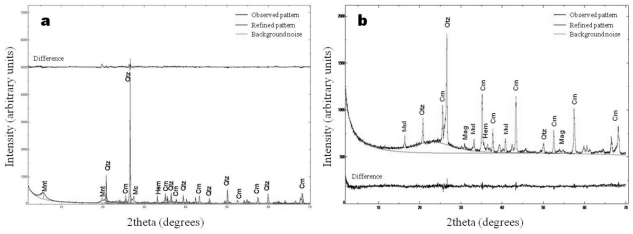

Figure 1. Refined XRD patterns of (a) natural clinker and (b) fly ash

3.1.1. Refinement of natural clinker

Rietveld refinement was done by changing 52 parameters: scale factors, cell constants (*a,b,c*), background noise

parameters, and the resolution of middle wide parameters (*U,V,W*). Residual values obtained after the refinement of the crystallographic phases were: R_{WP} = 18.66% and R_P = 7.47%, revealing that the data obtained during the measure of the pattern are favorable, R_B = 3.36–11.67%, showing that the selected models for each phase are appropriate with regards to the space group, cell parameters, and atomic positions. The goodness-of-fit obtained after refinement is 2.00, indicating a good accuracy of the adjustment. The quantitative analysis of phases in the natural clinker reveals a high content of amorphous material, 46%; quartz (SiO_2), 25.4%; microcline ($KAlSi_3O_8$), 14.2%; Ca-montmorillonite ($Ca_2Al_4Si_8O_{24}$), 11.1%; and minor hematite (Fe_2O_3), 3.3%. Figure 1a illustrates the refinement for NC. The difference between the experimental and calculated XRD patterns is shown in the bottom, showing good correlation.

3.1.2. Refinement of fly ash

Rietveld refinement was done as before by changing 41 parameters. The residual values obtained after the refinement of the crystallographic phases were: R_{WP} = 16.11%, R_P = 10.76%, R_B = 5.50 –13.64%, showing that the models selected for each phase are appropriate respect to space group, cell parameters, and atomic positions. The goodness-of-fit obtained after refinement is 1.39, indicating good accuracy for the adjustment.

The quantitative analysis of phases in the fly ash reveals a high content of amorphous material, 71%; mullite ($Al_{1.83}Si_{1.08}O_{4.85}$), 15.8%; quartz ($SiO_2$), 11.6%; minor magnetite (Fe_3O_4), 0.9%; and hematite (Fe_2O_3), 0.6%. Figure 1b illustrates the refinement for FA. The difference between the experimental and calculated XRD patterns is shown on the bottom, showing good correlation.

The SEM image (Fig. 2) reveals that NC displays a blocky morphology, while the particles of FA are predominantly spherical in shape with a relatively smooth surface texture.

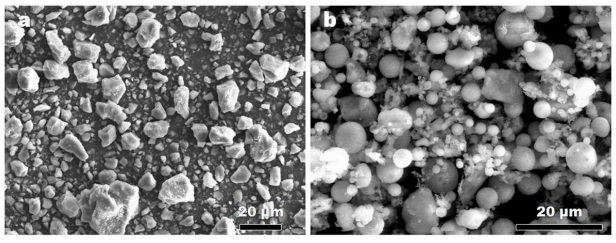

Figure 2. SEM images of (a) natural clinker and (b) fly ash

In Fig. 3, the infrared spectra Fourier Transformed for the raw materials are illustrated. The vibration bands at 1641 and 1635 cm^{-1} show the presence of water in the raw materials (H_2O deformation mode). Moreover, there are vibration bands, which are characteristic of aluminosilicates. The bands at 1032 and 1094 cm^{-1} are attributed to asymmetric stretching vibrations T-O (T = Si or Al); the bands at 700, 782, and 790 cm^{-1} are attributed to symmetric stretching vibrations T-O. These vibration bands can be due to the presence of quartz in natural clinker. The bands at 540 and 489 cm^{-1} can be attributed to octahedral aluminium in natural clinker and fly ash, respectively, and are due to octahedral aluminium [28].

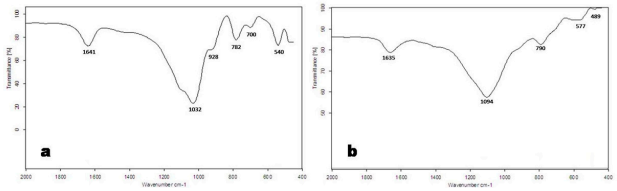

Figure 3. FTIR spectra for (a) natural clinker and (b) fly ash

3.2. Faujasite-type low-SiO_2 zeolite

The main as-synthesized zeolite obtained by the alkaline fusion followed by hydrothermal reaction method include: faujasite, sodalite, phillipsite, and chabazite. The synthesis of faujasite was investigated by the evaluation of some parameters affecting their formation process, such as the mineralogical composition of the starting material, reaction temperature, and time.

3.2.1. Synthesis of faujasite-type zeolite from natural clinker

Figure 4 shows the effect of reaction temperature and time after carrying out the fusion of natural clinker with NaOH followed by hydrothermal treatment. Faujasite was the main crystalline phase obtained, with phillipsite as a secondary phase. Figure 4a illustrates XRD profiles of the synthesis products obtained at 65 ºC. After 12 h of reaction, natural clinker does not show an effective transformation. After 24 h of reaction, several characteristic peaks of faujasite start to appear at 2θ of 6.093, 9.986, 15.40, and 26.66, which progressively increase in intensity after 48 h of reaction, with the appearance of weak peaks of phillipsite at 2θ of 12.41, 17.69, and 28.07. Figure 4b illustrates the XRD profiles

of the synthesis products obtained at 80 ºC. After 12 h of reaction, only faujasite appeared in the synthesis product. After 24 h of reaction, phillipsite appeared accompanying faujasite. With reaction time, faujasite shows an increase in intensity whereas phillipsite progressively decrease. At 95 ºC, both faujasite and phillipsite appear in the synthesis products.

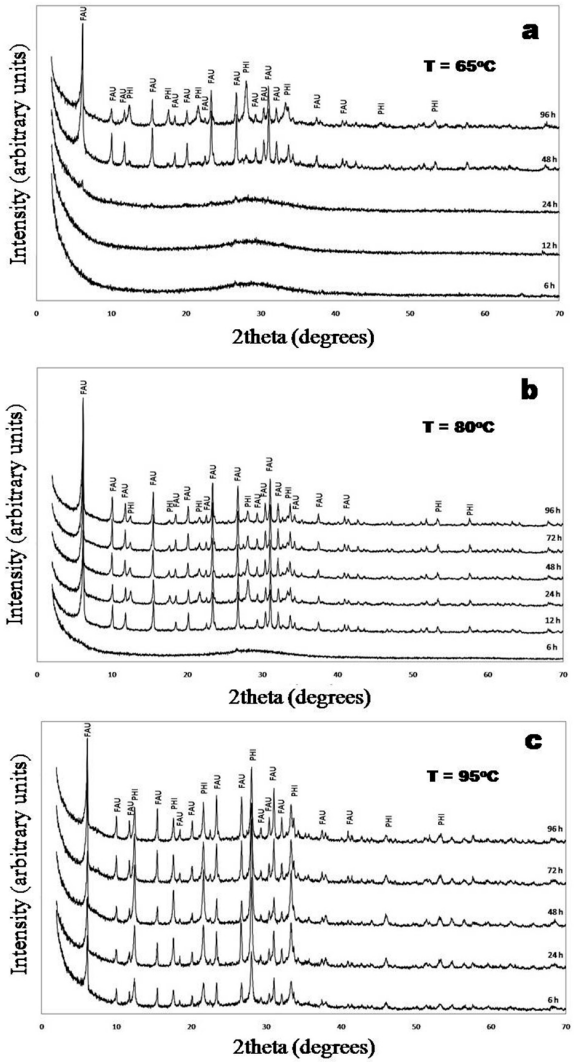

Figure 4. XRD patterns of as-synthesized products from natural clinker

3.2.2. Synthesis of faujasite-type zeolite from fly ash

Figure 5 shows the effect of reaction temperature and time after carrying out the fusion of fly ash with NaOH followed by hydrothermal treatment. Results reveal that the use of fly ash as starting material in the synthesis of zeolites was not very effective compared with those obtained using natural clinker. After 72 h of reaction, faujasite with low intensity peaks formed. After 96 h of reaction, faujasite with minor chabazite coexist. At 80 and 95 ºC, a mixture of several zeolitic products such as faujasite, with minor chabazite and sodalite was obtained. At 80 ºC with reaction time, the amount of faujasite and sodalite increases, with chabazite formation at 72 h of reaction time. At 95 ºC the characteristic peaks of faujasite reach the maximum intensity after 48 h, and then decrease. The amount of sodalite initially formed after 6 h of reaction decreases up to 48 h and then increases.

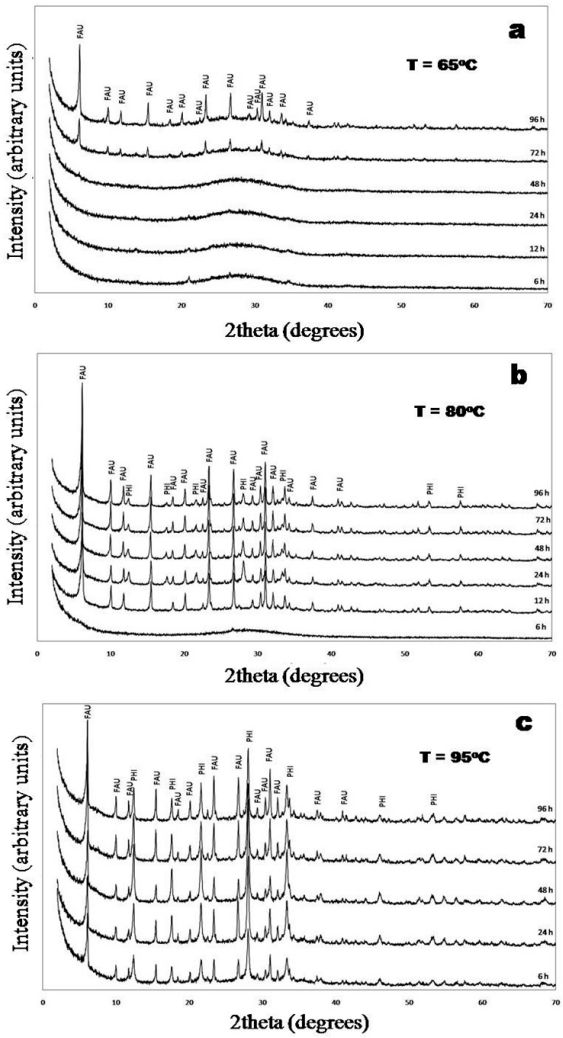

Figure 5. XRD patterns of as-synthesized products from fly ash

According to these results, the optimum experimental conditions for the synthesis of faujasite-type zeolite using the alkaline fusion method were: at 80 ºC after

12 h using natural clinker (FAU-1) and at 65 ºC after 96 h using fly ash (FAU-2) as starting materials. XRD profiles of the as-synthesized faujasite obtained at these experimental conditions and that for a commercial faujasite are shown in Fig. 6.

From the optimum experimental conditions, the one corresponding to the natural clinker-based faujasite was selected as the best result obtained in this study, taking into account the absence of additional crystalline phases and the short reaction time. Therefore, these conditions were used to discuss the formation process of faujasite.

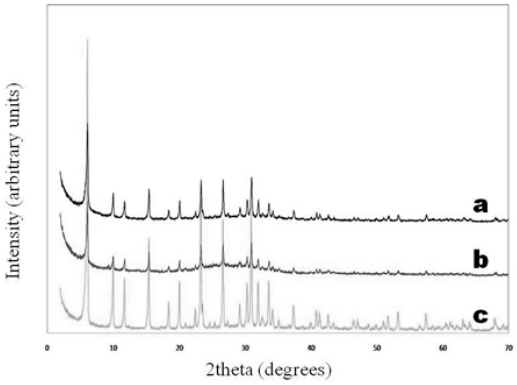

Figure 6. XRD patterns for (a) natural clinker-based, (b) fly ash-based, and (c) commercial faujasite

3.2.3. Fourier transformed infrared spectroscopy (FTIR)

The best synthesis products were also characterized by Fourier transformed infrared spectroscopy in order to obtain additional information on the crystalline structure of the as-synthesized faujasite. FTIR spectra of the selected synthesis products are illustrated in Fig. 7.

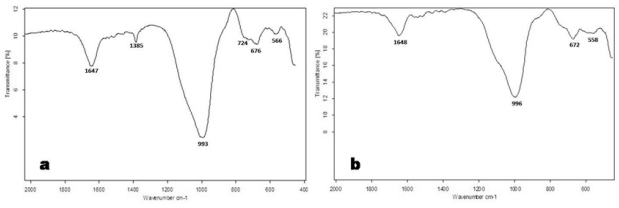

Figure 7. FTIR spectra for (a) natural clinker-based faujasite at 80 ºC for 12 h and (b) fly ash-based faujasite at 95 ºC for 96 h

The vibration bands at 1647 and 1648 cm^{-1} show that complete dehydration was not obtained in the synthesis products (H_2O deformation mode). The vibration bands at 993 and 996 cm^{-1} are attributed to the asymmetric stretching $_{vibrations}$ T-O (T = Si or Al). The vibration bands at 676 and 672 cm^{-1} are attributed to symmetric stretching $_{vibrations}$ T-O. The vibration bands at 566 and 558 cm^{-1} are due to D6R secondary structures in faujasite.

3.2.4. Scanning Electron Microscopy (SEM)

Figure 8 illustrates some SEM images of representative zeolitic products obtained in this study. In general, faujasite shows an octahedral morphology and sometimes penetration twinning. However, it is common to observe agglomerates of particles of faujasite-type zeolite with irregular morphology, sometimes accompanied by spheroidal aggregates of disk-shape sodalite.

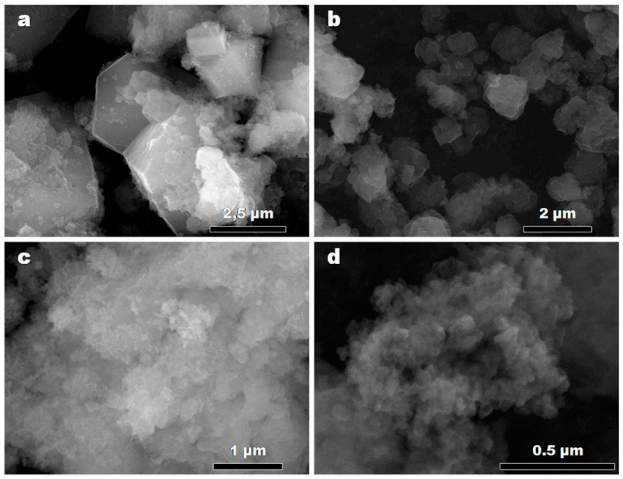

Figure 8. SEM images of the as-synthesized faujasite from (a-b) natural clinker and (c-d) fly ash

3.3. Reaction mechanism during faujasite-type zeolite synthesis

The reaction mechanisms of zeolite synthesis from coal by-products by alkaline fusion prior to hydrothermal reaction is discussed here and can be divided into a number of steps which are discussed along with Fig. 9. The chemistry of the evolution of the system is very complex due to several factors, such as: the formation of intermediate metastable phases, the occurrence of simultaneous reactions such as the precipitation and

dissolution of a gel phase, nucleation and growth of zeolitic phases of poor crystallinity, the dissolution of the early metastable phases, and the nucleation (and growth) of more stable phases. However, the reaction history of zeolite synthesis can be summarized as follows: As mentioned above, the optimum experimental conditions during the synthesis of faujasite-type zeolite were a reaction temperature and time of 80 ºC and 12 h, respectively, during hydrothermal treatment using natural clinker as the starting material. The steps to evaluate are: fusion of the starting material with NaOH, the preparation of the reaction gel, and a hydrothermal reaction at 80 ºC for 12 h.

Finally, we discuss several chemical reactions that can be involved in the synthesis of faujasite from natural clinker using the alkaline fusion step prior to the hydrothermal treatment. Figure 10 illustrates the faujasite forming reactions.

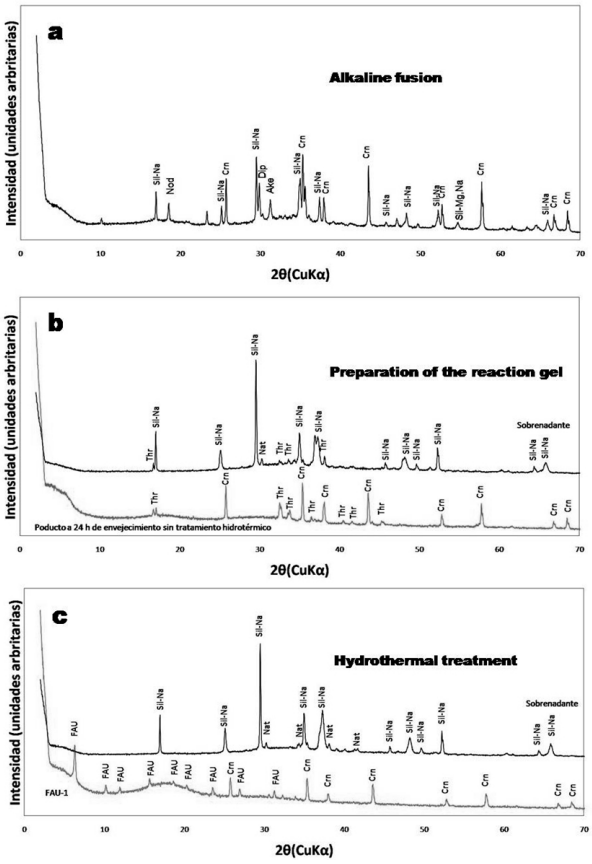

Figure 9. XRD patterns of the (a) fusion product between natural clinker and NaOH, (b) aged reaction gel and solid in the filtrate, and (c) faujasite synthesized from natural clinker at 80 ºC for 12 h and the solid in the filtrate

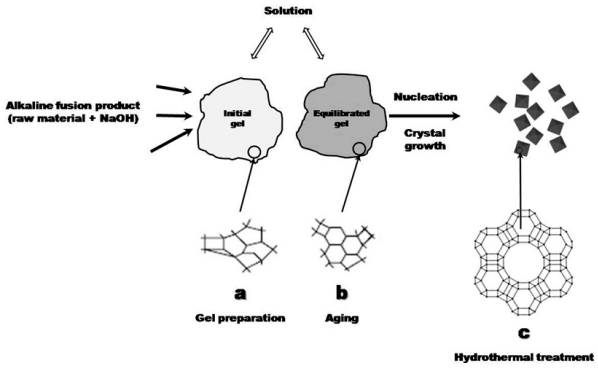

Figure 10. Faujasite-forming reactions [32]

3.3.1. Alkaline fusion

During the alkaline fusion step, a solid-state reaction between the alkaline activator (NaOH) and the crystalline phases of natural clinker occurred. As a result, most of the natural clinker particles can be converted into sodium silicate and aluminate salts at the fusion temperature (600 °C). This is summarized in reaction (1). Newly-formed compounds dissolved in water more readily than the mineral phases (quartz, hematite, microcline, and montmorillonite) in the starting material, which have a low velocity of dissolution with the occurrence of some of them as relict phases in the synthesis products.The main phases formed after fusion correspond to silicates (Fig. 10a) with minor amounts of other phases. These silicates along with $AlOH_3$ are the precursors for the synthesis of faujasite. Sodium silicate formed after fusion can be easily dissolved in H_2O.

(1) $NaOH_{(excess)} + Na_{0.3}(Al,Mg)_2Si_4O_{10}(OH)_2.4H_2O + SiO_2 + K(Si_{0.75}Al_{0.25})_4O_8 + Fe_2O_3 + \textit{Amorphous material} \xrightarrow{600\,^{\circ}C} Na_2SiO_3 + Al(OH)_3 + Ca_2Mg(Si_2O_7) + Ca(Mg_{82}Fe_{18})(Si_2O_6) + Na_2Mg(SiO_4) + CaMg(CO_3)_2 + \textit{Amorphous material}$

The quantitative analysis of the fusion product shows that it is composed of amorphous material, 50.1%; and crystalline phases, such as sodium silicate, Na_2SiO_3, 11.1%; nordstrandite, $Al(OH)_3$, 3.9%; akermanite, $Ca_2Mg(Si_2O_7)$, 7.1%; ferroan diopside, $Ca(Mg_{82}Fe_{18})(Si_2O_6)$, 12.9%; magnesium and sodium silicate, $Na_2Mg(SiO_4)$, 12.4%; and dolomite $CaMg(CO_3)_2$, 2.4%.

3.3.2. Preparation of the reaction gel

An H_2O/alkaline fused material ratio of 5 mL/g was used for the preparation of the hydrogel, which was kept mixing under magnetic stirring for 1 h. Then, it was aged for 24 h under static conditions. Aging was carried out to decrease the reaction time for faujasite synthesis. In the preparation step for the reaction gel and aging, $Al(OH)_3$ formed during the fusion step reaction with NaOH to form sodium aluminate, which reacts with silicates to produce the reaction gel, as summarized in reaction (2). During this step, the solid was separated from the filtrate by filtration. The solid is composed of thermonatrite ($Na_2CO_3.H_2O$) and amorphous material. The filtrate is mainly composed of sodium silicate with minor thermonatrite (Fig. 10b). Results reveal that sodium silicate formed during the fusion stage is dissolved and therefore it is found in the liquid phase. For the formation of faujasite in the hydrothermal reaction, the requested aluminum is supplied by $Al(OH)_3$ formed during the fusion stage, being in the amorphous material that forms part of the solid phase.

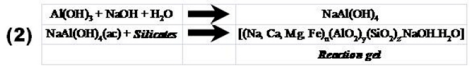

The quantitative analysis of the reaction gel reveals that it is manly composed of thermonatrite ($Na_2CO_3.H_2O$), 15.5%. The amount of amorphous material was 84.5%.

3.3.3. Hydrothermal treatment

During the synthesis of faujasite, the following events occur: an induction period, nucleation, and crystal growth [32]. The induction period is the time between the beginning of the reaction and the moment when the crystalline product is detected. Therefore, it starts in the preparation of the reaction gel (t = 0) and finishes when the zeolitic product is detected by XRD. The induction time is followed by the processes of nucleation and crystal growth. The dissolution of sodium silicate released ionic species which were transported to the nucleation sites. As the condensation of aluminate and silicate ions took place, the precipitation of an aluminosilicate gel occurs. Nucleation is the phase transition by which a critical volume of a semi-ordered gel is transformed in a structure sufficiently ordered to form a growth center from which the crystalline structure can propagate. A polymerization should be the process that forms the zeolitic precursors, which contains tetrahedra of Si and Al randomly distributed along the polymeric chains that are cross-linked so as to provide cavities sufficiently large to accommodate the charge-balancing alkali ions. The formation of different nucleation sites occurred and, following the Ostwald rule, larger crystallites (usually with lower surface free energy contribution and more stable) destabilized smaller coexisting crystals of the same phase, decreasing crystal size distribution and promoting the growth of progressively zeolite crystals. Crystallization generally involved the assimilation of material from the solution by a growth process, which began when the nuclei reached a critical size and the crystals started to grow. Crystal growth occurs during the hydrothermal reaction. A stable phase reached the required equilibrium conditions to promote the crystal growth of the faujasite-type zeolite. The lineal growth rates of zeolites show a strong dependence on temperature. However, these rates are also influenced by several variables, particularly the molar composition of the reaction gel. In the case of faujasite, the growth rate decreases when the content of the SiO_2 of the product increases.

The hydrothermal treatment of the reaction gel at the schedule temperature and time of reaction produced the crystallization of faujasite. Taking into account that the starting material presents Na and other metals such as Ca and Mg, which form part of the silicates formed during the fusion step, they can be part of the as-synthesized faujasite structure. On the other hand, as mentioned above, the synthesis was carried out with raw materials with large amounts of amorphous material, which still remains in the final product, and therefore it is difficult to establish the stechiometry of the reaction occurred at this step. On the other hand, the chemical composition and Si/Al ratio of the as-synthesized faujasite are not known. However, we proposed reaction (3) to explain the transformation of the reaction gel into faujasite.

Figure 10c illustrates the occurrence of faujasite (FAU-1) with amorphous material. Sodium silicate still remains in the filtrate. Therefore, it is very important

to do the variation of the Si/Al ratio of the starting material, taking into account that it would increase the growth rates of faujasite with the benefit of obtaining residual silicate.

By this method, both crystalline and amorphous materials in natural clinker were converted into soluble compounds that promote the formation of faujasite and avoid the presence of relict crystalline phases of the starting materials in the as-synthesized products.

4. CONCLUSIONS

The conversion of coal by-products into zeolites both contributes to the mitigation of environmental problems and turns this by-product of the coal industry into an attractive and useful material. Zeolitic materials were successfully synthesized via hydrothermal treatment and alkaline fusion followed by hydrothermal reaction using both NC and FA as starting materials and NaOH as an alkaline activator. In some cases, zeolite formation was assessed to be fairly unsuccessful, taking into account that the synthesis products contain a substantial percentage of hydroxysodalite, with some quartz and mullite also present, while only a very small fraction of a desired zeolitic phase can be observed. Several types of zeolitic material can be obtained according to experimental conditions. Our experimental data suggest that coal by-products could be converted into a beneficial product, which could be used in the future as ion exchangers. Therefore, it is necessary to develop further experiments under well-optimized conditions to successfully prepare highly-crystalline zeolites. The efficiency in the conversion of coal by-products can be affected by the contents of non-reactive phases (mainly mullite and quartz) or glass as well as its grain size distribution. Preliminary results reveal that the production of crystalline faujasite-type zeolite as the main component and other minor phases, can show adsorbent and ion-exchange properties with a wide spectrum of applications.

ACKNOWLEDGMENTS

This research forms part of the undergraduate thesis of J. Oviedo and has benefited from research facilities provided by the *Universidad Industrial de Santander*, the *Centro de Desarrollo Productivo de Joyería de Bucaramanga* and the *Instituto Zuliano de Investigaciones Tecnologicas*. We thank Andelfo Pinilla, Mario Macías, and Eric Plaza for their assistance with the XRD, XRF, and SEM data acquisition.

REFERENCES

[1] Höller, H., Barth-Wirsching, U., Zeolite formation from fly ash. Fortschr. Miner. 63, pp. 21-43, 1985.

[2] Ríos, C., Williams, C., Castellanos, O., Synthesis and characterization of zeolites by alkaline activation of kaolinite and industrial by-products (fly ash and natural clinker). Bistua 4, pp. 60-71, 2006.

[3] Mondragón, F., Rincón, F., Sierra, L., Escobar, J., Ramírez, J., Fernández, J., New perspectives for coal ash utilization: Synthesis of zeolitic materials. Fuel 69, pp. 263-266, 1990.

[4] Kolousek, D., Seidl, V., Prochazkova, E., Obsasnikova, J., Kubelkova, L., Svetlik, L., Ecological utilization of power-plant fly ashes by their alteration to phillipsite: hydrothermal alteration, application. Acta Univ. Geol. 37, pp.167-178, 1993.

[5] LIN, C.-F., HIS, H.-C., Resource recovery of waste fly ash: Synthesis of zeolite-like materials. Environ. Sci. Technol. 29, pp. 1109-1117, 1995.

[6] Park, M., Choi, J., Synthesis of phillipsite from fly ash. Clay. Sci. 9, pp. 219-229, 1995.

[7] Shih, W.-H., Chang, H.-L., Shen, Z., Conversion of class-F fly ash to zeolites. Mater. Res. Soc. Symp. Proc. 371, pp. 39-44, 1995.

[8] Amrhein, C., Haghnia, G.H., Kim, T.S., Mosher, P.A., Gagajena, R.C., Amanios, T., De La Torre, L., Synthesis and properties of zeolites from fly ash. Environ. Sci. Technol. 30, pp. 735-742, 1996.

[9] Querol, X., Plana, F., Alastuey, A., Lopez-Soler, A., Synthesis of Na-zeolites from fly ash. Fuel 76, pp. 793-799, 1997.

[10] Rayalu, S., Meshram, S.U., Hasan, M.Z., Highly crystalline faujasitic zeolites from fly ash. J. Hazard. Mater. 77, pp. 123-131, 2000.

[11] Querol, X., Moreno, N., Umaña, J.C., Alastuey, A., Hernández, E., López-Soler, A., Plana, F., Synthesis of zeolites from fly ash: an overview. Int. J. Coal. Geol. 50, pp. 413-423, 2002.

[12] Murayama, N., Yamamoto, H., Shibata, J., Mechanism of zeolite synthesis from coal fly ash by alkali hydrothermal reaction. Int. J. Miner. Process. 64, pp. 1-17, 2002.

[13] Mouhtaris, Th., Charistos, D., Kantiranis, N., Filippidis, A., Kassoli-Fournaraki, A., Tsirambidis, A. GIS-type zeolite synthesis from Greek lignite sulphocalcic fly ash promoted by NaOH solutions. Microporous Mesoporous Mater. 61, pp. 57–67, 2003.

[14] Ojha, K., Pradhan, N.C., Samanta, A.N., Zeolite from fly ash: synthesis and characterization. Bull. Mater. Sci. 27, pp. 555-564, 2004.

[15] Inada, M., Eguchi, Y., Enomoto, N., Hojo, J., Synthesis of zeolite from coal ashes with different silica–alumina composition. Fuel 84, pp. 299–304, 2005.

[16] Ríos, C.A., Williams, C.D., Roberts, C.L., A comparative study of two methods for the synthesis of fly ash-based sodium and potassium type zeolites with potential use in the purification of wastewaters. Fuel 88, pp. 1403-1416, 2009.

[17] Shigemoto, N., Hayashi, H., Miyaura, K., Selective formation of Na-X zeolite from fly ash by fusion with sodium hydroxide prior to hydrothermal reaction. J. Mater. Sci. 28, pp. 4781-4786, 1993.

[18] Ríos, C.A, Williams, C.D., Synthesis of zeolitic materials from natural clinker: A new alternative for recycling coal combustion by-products. Fuel 87, pp. 2482-2492, 2008.

[19] Querol, X., Plana, F., Alastuey, A., Lopez-Soler, A., Andres, J.M., Juan, R., Ferrer, P., Ruiz, C.R., A fast method of recycling fly ash: Microwave assisted zeolite synthesis. Environ. Sci. Technol. 31, pp. 2527-2532, 1997.

[20] Park, M., Choi, C.L., Lim, W.T., Kim, M.C., Choi, J., Heo, N.H., Molten-salt method for the synthesis of zeolitic materials: I. Zeolite formation in alkaline molten-salt system. Microporous Mesoporous Mater. 37, pp. 81-89, 2000.

[21] Park, M., Choi, C.L., Lim, W.T., Kim, M.C., Choi, J., Heo, N.H., Molten-salt method for the synthesis of zeolitic materials: II. Characterization of zeolitic materials. Microporous Mesoporous Mater. 37, pp. 91-98, 2000.

[22] Hollman, G.G., Steenbruggen, G., Janssen-Jurkovičová, M., A two-step process for the synthesis of zeolites from coal fly ash. Fuel 78, pp. 1225-1230, 1999.

[23] Moreno, N., Querol, X., Andrés, J.M., López-Soler, A., Janssen-Jurkovičová, M., Nugteren, H., Towler, M., Stanton, K., Determining suitability of a fly ash for silica extraction and zeolite synthesis. J. Chem. Tech. and Biotech. 79, pp. 1009-1018, 2004.

[24] Moreno, N., Querol, X., Ayora, C., Fernández-Pereira, C., Janssen- Jurkovičová, M., Utilisation of zeolites synthesized from fly ash for the purification of acid mine waters. Environ. Sci. Technol. 35, pp. 3526-3534, 2001.

[25] Moreno, N., Querol, X., Ayora, C., Alastuey, A., Fernández-Pereira, C., Janssen-Jurkovičová, M. Potential environmental applications of pure zeolitic material synthesized from fly ash. J. Environ. Eng. 127, pp. 994-1002, 2001.

[26] Querol, X., Moreno, N., Umaña, J.C., Juan, R., Hernández, S., Fernandez-Pereira, C., Ayora, C., Janssen-Jurkovičová, M., García-Martínez, J., Linares-Solano, A., Cazorla-Amoros, D., Application of zeolitic material synthesized from fly ash to the decontamination of waste water and flue gas. J. Chem. Tech. and Biotech. 77, pp. 292-298, 2002.

[27] Ríos, C.A., Williams, C.D., Roberts, C.L., Removal of heavy metals from acid mine drainage (AMD) using coal fly ash, natural clinker and synthetic zeolites. J. Haz. Mater. 156, pp. 23-35, 2008.

[28] Ríos, C., Synthesis of zeolites from geological materials and industrial wastes for potential application in environmental problems. PhD thesis, University of Wolverhampton, United Kingdom, 2008.

[29] Sandoval, M.V., Henao, J.A., Ríos, C.A., Williams, C.D., Apperley, D.C., Synthesis and characterization of zeotype ANA framework by hydrothermal reaction of natural clinker. Fuel 88, pp. 272-281, 2009.

[30] Vassilev, S.V., Vassileva, C.G., A new approach for the classification of coal fly ashes based on their origin, composition, properties, and behaviour. Fuel 86, pp. 1490-1512, 2007.

[31] Pinilla, A., Use of the combined RIR-Rietveld method of X-ray diffraction for the quantitative analysis of crystalline phases with or without amorphous material in polycrystalline samples. Undergraduate thesis, Universidad Industrial de Santander, Colombia, 2005.

[32] Cundy, C.S., Cox, P.A., The hydrothermal synthesis of zeolites: Precursors, intermediates and reaction mechanism. Microporous Mesoporous Mater. 82, pp. 1-78, 2005.